*Advances in Computational Mathematics* **16:** 263–290, 2002.


# Differential operators on graphs and photonic crystals

P. Kuchment [a,*] and L. Kunyansky [b]

[a] *Department of Mathematics and Statistics, Wichita State University, Wichita, KS, and Math. Dept., Texas A&M University, College Station, TX 77543, USA*
E-mail: kuchment@math.tamu.edu

[b] *ACM, Caltech, Pasadena, CA, USA, and Department of Mathematics, University of Arizona, Tucson, AZ, USA*
E-mail: leonk@math.arizona.edu

Received 12 April 2001
Communicated by C.A. Micchelli

Studying classical wave propagation in periodic high contrast photonic and acoustic media naturally leads to the following spectral problem: $-\Delta u = \lambda \varepsilon u$, where $\varepsilon(x)$ (the dielectric constant) is a periodic function that assumes a large value $\varepsilon$ near a periodic graph $\Sigma$ in $\mathbb{R}^2$ and is equal to 1 otherwise. High contrast regimes lead to appearence of pseudo-differential operators of the Dirichlet-to-Neumann type on graphs. The paper contains a technique of approximating these pseudo-differential spectral problems by much simpler differential ones that can sometimes be resolved analytically. Numerical experiments show amazing agreement between the spectra of the pseudo-differential and differential problems.

**Keywords:** photonic bandgap, photonic crystal, spectrum, Dirichlet-to-Neumann map, differential operators on graphs, pseudo-differential operators on graphs

## 1. Introduction

Photonic crystals are composite materials of periodic structure; they can be viewed as optical analogs of semi-conductors [45,71]. Introduction of these materials promises to bring about revolutionary changes in many areas of technology (lasers, computers, information transmission, etc.). The reader can find the relevant physics surveys in [10,15,39,44,53,57,58,69,70] and a survey of mathematical issues involved in [50]. Acoustic analogs of photonic crystals are also of significant interest. One of the major topics in photonic crystals theory and its acoustic analog is numeric and analytic study of the spectral structure of such materials. In particular, one of the principal issues is existence of spectral gaps. However, spectral analysis of such complex materials is rather hard [50]. It has been noticed, though, that high contrast thin structures (like thin optically dense dielectric walls surrounding air voids) favor spectral gaps. Although direct

* Work of both authors was partially supported by the NSF Grant DMS 9610444 and by a DEPSCoR Grant. Work of the first author was also supported by the NSF Grant DMS 0072248.

analysis of such media might seem even more complicated, one hopes that they could be approximately described by models of lower dimension that would be more willing to submit to analysis. Indeed, such approximate models are widely used in theory of mesoscopic systems [3,16,17,35–37,40,43,68] where electron propagation in quantum wire circuits can often be described by simplified one-dimensional models on graphs [1,5,22–24,52,60–64,66]. As it was shown in [6,7,25,27–31,50,51], a somewhat similar spectral behavior can be observed in the photonic crystal situation. Namely, in the case of $2D$ thin high contrast dielectric structures the electromagnetic waves in a photonic crystal split into two classes: the "air" waves that essentially concentrate in the air and bounce off the dielectric walls, and "dielectric" waves that use the thin dielectric walls as a waveguide for propagation. While the spectral structure of the air waves is rather simple and nice (with wide gaps opening), the dielectric waves lead to much more complex spectra. It was shown in [30] that propagation of these waves can be approximately described by a pseudo-differential operator (Dirichlet to Neumann map) on the graph $\Sigma$ that reflects the geometry of the material. Such representation is simpler, and of lower dimension than the original problem, thus allowing one to conduct a more thorough analysis of spectra. In particular, the possibility of opening spectral gaps was analytically proven in [27,28] using this model. However, due to the pseudo-differential nature of such approximation the corresponding spectrum often can not be found analytically; solution of the problem still requires considerable numerical computations.

It was noticed in [51] (see also [7,50]) that in certain cases one can make one more step of approximation and reduce the pseudo-differential problem to a differential one; the latter can then be studied analytically, or even solved explicitly. In the above mentioned works such a reduction to a differential problem was achieved in the restricted case of a smooth structure (which means in particular that the graph could not have vertices of valence higher than two); more practically interesting cases were not considered. The aim of this paper is to develop a (partially heuristic) technique that enables one to reduce the pseudo-differential problem to a differential one in more general non-trivial situations. As shown in the present paper, some of the resulting differential problems can then be resolved analytically, others require little numerical effort, such as finding roots of a 1-D function (in contrast with the boundary element type approaches required for the pseudo-differential problem). We provide numerical evidence of an amazing agreement between the spectra of the differential models and the spectra of the corresponding pseudo-differential models that they approximate. Such a close agreement confirms that the heuristic steps involved in our derivation do make sense.

We would also like to mention other situations ranging from scattering theory to tomography, to averaging in dynamical systems, to spectral theory, to study of effects related to non simple connectedness of physical systems (like the Aharonov–Bohm effect), where similar differential models on graphs have been used recently [4,5,9, 11–14,20,21,32–34,47,48,54–56,65].

The paper is structured as follows. The next section sets up the mathematical model of the problem under investigation. Section 3 contains the main analysis. Here we study the vertex behavior of the eigenmodes of the Dirichlet-to-Neuman operator on a graph under the assumption of symmetry of all junctions. The discovered behavior is then used in section 4 to prescribe boundary conditions for a differential problem on the graph. Due to space limitations, we treat here only examples of graphs with symmetric triple junctions at the vertices (such as, for instance, the honeycomb structure shown in figure 3). The numerical results are provided showing an extraordinary agreement of spectra and of dispersion curves for the differential and the original pseudo-differential problem. Study of some other interesting geometries, as well as of additional spectral effects are left for a future publication. Sections 4 and 5 are devoted to final remarks and conclusions and to acknowledgements.

## 2. Setting up the model

We will restrict our analysis to the case of 2D photonic crystals and EM waves propagating along the periodicity plane. In this case there are two possible polarizations (see [42,44]). We will be interested in the one where the electric field $E$ is perpendicular to the plane of periodicity ($E$-fields). As it was shown in [27,28] (see also [25,50]), this is the only polarization that in the case of high contrast thin structures leads to "dielectric" modes. The wave propagation in this case is described by the following scalar eigenvalue problem in 2D

$$-\Delta E = \lambda\varepsilon(x)E, \tag{1}$$

where $\lambda = (\omega/c)^2$, $\omega$ is the frequency of the wave, $c$ is the speed of light, and $\varepsilon(x)$ is the (periodic) electric permittivity function in the plane.

The dielectric function $\varepsilon(x)$ is assumed to have the following structure. A periodic graph $\Sigma$ on the plane represents the geometry of the material. Namely, a dielectric with a high value of the dielectric constant $\varepsilon$ occupies a neighborhood of width $d \ll 1$ of $\Sigma$, and the rest is filled with the air (dielectric constant 1). In other words, $\varepsilon(x)$ is equal to $\varepsilon \gg 1$ in a $d$-neighborhood of $\Sigma$ and $\varepsilon(x) = 1$ otherwise. An example of a cross-section of such 2-D structure is shown in figure 1; the dark areas in the picture represent dielectric, while the rest of the structure is filled with air.

The following result was obtained in [28,30] (see also [7,50]). Assume that $d \to 0$ and $\varepsilon d \to \infty$. Let us zoom in on the spectrum of the problem (1) by multiplying $\lambda$ by large parameter $\varepsilon d$. After this rescaling, the spectrum of (1) converges to the spectrum of the Helmholtz type problem

$$-\Delta u = \lambda\delta_\Sigma u. \tag{2}$$

Here $\delta_\Sigma(x)$ is the delta-function supported by the graph $\Sigma$ (i.e., $\langle\delta, \phi\rangle = \int_\Sigma \phi(x)\,\mathrm{d}x$). Equation (2) can be understood as follows: function $u$ is harmonic outside graph $\Sigma$, continuous through $\Sigma$, and the jump of its normal derivatives across $\Sigma$ is proportional (with a factor $\lambda$) to the values of $u$ on $\Sigma$. In other words (see details in [30,51]), problem (2) is equivalent to the spectral problem

$$\Lambda_\Sigma u = \lambda u, \tag{3}$$

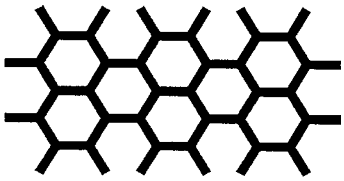

Figure 1. The cross-section of a 2D thin photonic crystallic structure. The dark areas are filled with an optically dense dielectric with the dielectric constant $\varepsilon$, while the white ones represent the air ($\varepsilon = 1$).

where $\Lambda_\Sigma$ is the Dirichlet-to-Neumann operator on the graph $\Sigma$. This operator takes a function $u$ on $\Sigma$, uses it as the Dirichlet boundary data for finding a harmonic function in $\mathbb{R}^2 \backslash \Sigma$, and then produces the jump of the normal derivative of this function across $\Sigma$. One can easily establish [51] that $\Lambda_\Sigma$ is a pseudo-differential operator of first order along smooth parts of $\Sigma$, whose full (rather than just the principal) symbol is $2|\xi|$. This fact implies that when $\Sigma$ is smooth, the spectrum of $\Lambda_\Sigma$ for large $\lambda$ behaves asymptotically as $2\sqrt{\lambda_n}$, where $\lambda_n$ are the eigenvalues of the second derivative operator $(-\mathrm{d}^2/\mathrm{d}l^2)$ with respect to the arc length along $\Sigma$. Such an asymptotic spectral behavior allows one to obtain simple and often very good estimates of the spectrum [51]. It also simplifies certain theoretical considerations, since spectra of differential (rather than pseudo-differential) problems on graphs submit much more readily to analysis.

The main observation made above was that a certain power (namely, square) of the Dirichlet-to-Neumann operator $\Lambda_\Sigma$ can be approximated nicely (up to a smoothing operator) by a differential operator on $\Sigma$. However, this has been established for the restricted case of smooth $\Sigma$ only. Thus in this paper we consider a more interesting and practically important case of a graph $\Sigma$ that does have vertices, and hence singularities. Our goal is to find differential problems on $\Sigma$ that, under the above assumptions, provide approximations of the spectrum of $\Lambda_\Sigma$. Although there is still no complete understanding of this problem yet, we develop an heuristic analysis that for certain geometries results in differential problems yielding amazingly good approximations for spectra in question.

## 3. Differential operators on graphs

Given some periodic graph $\Sigma$ (whose edges will be assumed to be segments of straight lines), we are trying to find a differential operator whose spectrum provides high-frequency asymptotics to the spectrum of the Dirichlet-to-Neumann operator $\Lambda_\Sigma$ on $\Sigma$.

A natural candidate is the differential operator

$$A_M u = \frac{\mathrm{d}^{2M} u}{\mathrm{d}l^{2M}}, \tag{4}$$

where $l$ is the arc length coordinate along each of the edges of the graph and $M$ is a natural number. The corresponding spectral problem on each of the graph's edges will be written as

$$\frac{\mathrm{d}^{2M}}{\mathrm{d}l^{2M}} u(l) = \left(\mathrm{i}\frac{\lambda}{2}\right)^{2M} u(l). \tag{5}$$

The reason for the way the spectral problem is written is that along the smooth parts of the graph the operator $\Lambda_\Sigma$ "behaves like" $2\sqrt{-\mathrm{d}^2/\mathrm{d}l^2}$. More precisely, along the edges the sum $(\Lambda_\Sigma/2)^2 + \mathrm{d}^2/\mathrm{d}l^2$ is a smoothing operator [51]. This makes (5) the natural candidate for spectral approximation. However, neither the operator (4), nor the spectral problem (5) are defined until appropriate boundary conditions at the nodes and free ends of the graph $\Sigma$ are provided. These conditions at the vertices of the graph are the object of our investigation. So, our main question can be formulated now as follows:

*Can certain boundary conditions be supplied to (5) such that the resulting spectrum asymptotically for large $\lambda$ coincides with the spectrum of $\Lambda_\Sigma$?*

Here is how we approach this problem. We first analyze the vertex behavior of the eigenmodes of the Dirichlet-to-Neumann operator $\Lambda_\Sigma$. In particular, we conclude that the derivatives of the eigenmodes at the vertices (when the modes are sufficiently smooth) satisfy some mandatory linear relations. Then these relations are imposed as boundary conditions on (5). We discover, in particular, that in contrast with the smooth case, $M$ is not always equal to 1. For instance, for the square geometry one needs to use $M = 2$. Our analysis is based on a reliable heuristics rather than on rigorous proofs (although it probably could be made rigorous with a significant extra effort). In particular, we cannot show like we did in [51] in the smooth case that the difference $A_M - (\Lambda_\Sigma)^M$ is a smoothing operator. The problem is that one deals in this case with a singular variety $\Sigma$. However, when the spectra of $A_M$ and $(\Lambda_\Sigma)^M$ are compared numerically, they show miraculous agreement, which suggests validity of the derived results.

### *3.1. Vertex conditions for Dirichlet-to-Neumann eigenmodes on symmetric star structures*

In this section we will study the behavior near the graph's vertices of the eigenmodes of the Dirichlet-to-Neumann operator $\Lambda_\Sigma$. We will restrict consideration to the case of symmetric junction of $N$ edges at each vertex only. It is not clear at the moment what can be said about nonsymmetric junctions. Since vertex behavior of eigenmodes should depend on local values of the field only, we will work with a star structure consisting of a single vertex that joins $N$ edges of a finite length. Polar coordinates $(r, \varphi)$ will be used with the origin at the vertex and the polar axis that goes along the bisector of the angle between two adjacent edges. We denote by $\Phi = 2\pi/N$ the angle between two adjacent edges.

The spectral problem for the Dirichlet-to-Neumann operator will be written as

$$-\Delta V = \lambda \delta_\Sigma V, \tag{6}$$

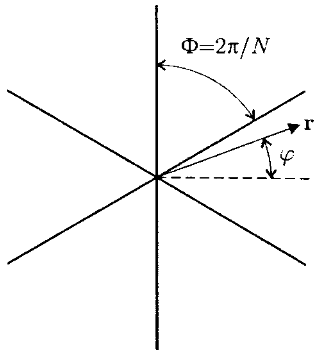


Figure 2. The symmetric $N$-edge star structure $\Sigma$.

where $\delta_\Sigma$ is the Dirac's delta-function supported on the symmetric $N$-edge star structure $\Sigma$:

$$\delta_\Sigma(r,\varphi) = \Theta(R-r)\Theta(r)\sum_{l=0}^{N-1}\delta\left(\varphi - \Phi l + \frac{\Phi}{2}\right), \quad R > 1.$$

Here $\Theta(r)$ is the Heaviside function:

$$\Theta(r) = \begin{cases} 0, & r < 0, \\ 1, & r \geqslant 0. \end{cases}$$

The cut-off function $\Theta(R-r)$ is utilized to model the finite length $R$ of the edges.

Due to the rotational symmetry of the structure with respect to the cyclic group $\mathbb{Z}_N$ of $N$th roots of the unity, we can look first at solutions that are transformed according to an irreducible representation of this group. There are $N$ series of such eigenmodes:

$$V_m(r,\varphi+\Phi) = V_m(r,\varphi)\mathrm{e}^{\mathrm{i}m\Phi}, \quad m = -\left[\frac{N}{2}\right],\ldots,\left[\frac{N}{2}\right], \tag{7}$$

where $[x]$ stands for the integer part of $x$. When $N$ is even, the conditions for $m = -[N/2]$ and $m = [N/2]$ are identical.

Due to our choice of polar coordinates, the star structure is mirror symmetric with respect to the polar axis. Therefore, it is sufficient to consider non-negative values $m = 0,\ldots,[N/2]$ only.

For a fixed $m$, symmetry conditions (7) enable us to re-write the problem (3) (or, equivalently, (6)) for the angular domain

$$\mathcal{A} = \left\{(r,\phi)\;\middle|\; -\frac{\Phi}{2} < \varphi < \frac{\Phi}{2},\; r > 0\right\}$$

only. Namely, we are looking for a function $V_m(r,\varphi)$ harmonic in $\mathcal{A}$ and satisfying the following two conditions (that correspond respectively to the continuity through $\Sigma$ and the jump of its normal derivative condition across $\Sigma$):

$$V_m\left(r,\frac{\Phi}{2}\right)\mathrm{e}^{-\mathrm{i}m\Phi/2}=V_m\left(r,-\frac{\Phi}{2}\right)\mathrm{e}^{\mathrm{i}m\Phi/2},\tag{8}$$

$$\mathrm{e}^{-\mathrm{i}m\Phi/2}\frac{\partial V_m}{\partial\varphi}\left(r,\frac{\Phi}{2}\right)-\mathrm{e}^{\mathrm{i}m\Phi/2}\frac{\partial V_m}{\partial\varphi}\left(r,-\frac{\Phi}{2}\right)=\lambda r\Theta(R-r)V_m\left(r,\frac{\Phi}{2}\right)\mathrm{e}^{-\mathrm{i}m\Phi/2}.\tag{9}$$

Notice the appearance of the factor $r$ in the right-hand side of (9), which is due to the relation $\partial/\partial n=r^{-1}\partial/\partial\phi$ between the normal derivative at a point of $\Sigma$ and the derivative with respect to the polar angle $\phi$. Let us denote the joint value of both sides of (8) by $w_m(r)$.

It is known that the radial Mellin transform (i.e., the Fourier transform in logarithmic coordinates) is a useful tool when studying the behavior of solutions of elliptic boundary value problems around corner points of the boundary (see, for instance, [38,46]). So, let us introduce a new variable $\rho=\ln r$. Denoting $v_m(\rho,\varphi)=V_m(\mathrm{e}^{\rho},\varphi)$, it is straightforward to check that the problem is reformulated as the equation in a strip

$$-\Delta v_m(\rho,\varphi)=0,\quad -\frac{\Phi}{2}<\varphi<\frac{\Phi}{2},\ -\infty<\rho<\infty,\tag{10}$$

where $\Delta$ denotes the Laplace operator in the $(\rho,\phi)$-plane, with the boundary conditions

$$v_m\left(\rho,\frac{\Phi}{2}\right)\mathrm{e}^{-\mathrm{i}m\Phi/2}=v_m\left(\rho,-\frac{\Phi}{2}\right)\mathrm{e}^{\mathrm{i}m\Phi/2}=w_m(\rho)\tag{11}$$

and

$$\mathrm{e}^{-\mathrm{i}m\Phi/2}\frac{\partial v_m}{\partial\varphi}\left(\rho,\frac{\Phi}{2}\right)-\mathrm{e}^{\mathrm{i}m\Phi/2}\frac{\partial v_m}{\partial\varphi}\left(\rho,-\frac{\Phi}{2}\right)=\lambda\mathrm{e}^{\rho}\Theta(\ln R-\rho)w_m(\rho).\tag{12}$$

We will be looking for a solution $V_m(r,\varphi)$ that is bounded in $\mathcal{A}$ and decays at infinity, for instance, as

$$V_m(r,\varphi)<\frac{C}{1+r^{\gamma}},\quad \gamma>0,\ r\to\infty.\tag{13}$$

We are interested in the behavior of this solution at $r=0$. Namely, we want to study the possibility of the Taylor representation

$$V_m\left(r,\frac{\Phi}{2}\right)\mathrm{e}^{-\mathrm{i}m\Phi/2}=\sum_{k=0}^{l}v_{m,k}r^k+\mathrm{O}\left(r^{l+\alpha}\right),\quad r\to0,\ \alpha>0.\tag{14}$$

If this is possible, we want to know as much as possible about the coefficients

$$v_{m,k}=\frac{1}{k!}V_m^{(k)}\left(0,\frac{\Phi}{2}\right)\mathrm{e}^{-\mathrm{i}m\Phi/2}.$$

Specifically, any mandatory linear relations between these coefficients are of interest. We will always assume continuity of the solution at the vertex, so (14) is assumed to hold for $l = 0$ with the values $v_{m,0}$ independent on $m$.

The expansion (14) can be rewritten in terms of $w_m(\rho)$:

$$w_m(\rho) = \sum_{k=0}^{l} v_{m,k} e^{k\rho} + O\bigl(e^{(l+\alpha)\rho}\bigr), \quad \rho \to -\infty, \ \alpha > 0. \tag{15}$$

Let us expand $w_m(\rho)$ into two parts supported on two half-axes:

$$w_m(\rho) = \bigl(1 - \Theta(\rho)\bigr) w_m(\rho) + \Theta(\rho) w_m(\rho) = w_{m,0}(\rho) + w_{m,1}(\rho). \tag{16}$$

I.e.,

$$w_{m,0}(\rho) = \begin{cases} w_m(\rho), & \rho < 0, \\ 0, & \rho \geqslant 0, \end{cases}$$
$$w_{m,1}(\rho) = \begin{cases} 0, & \rho < 0, \\ w_m(\rho), & \rho \geqslant 0. \end{cases}$$

Taking now the Fourier transform (which amounts to the Mellin transform in the original variable $r$) and using (15), we get

$$\widehat{w}_{m,0}(\xi) = \frac{i}{\sqrt{2\pi}} \sum_{k=0}^{l} \frac{v_{m,k}}{\xi + ik} + A(\xi), \tag{17}$$

where $A(\xi)$ is analytic for $\operatorname{Im}\xi > -(l + \alpha)$. On the other hand, due to (13) $\widehat{w}_{m,1}(\xi)$ is analytic in the half-plane $\operatorname{Im}\xi < \gamma$. We therefore conclude that possibility of a Taylor representation (14) boils down to existence of simple poles of the Mellin transform $\widehat{w}_{m,0}(\xi)$ at the points $-ik$ for $k = 0, \ldots, l$, with the residues equal (up to the constant factor $i/\sqrt{2\pi}$) to the radial derivatives of the original function at $r = 0$. Existence of higher order poles would therefore indicate that the Taylor expansion breaks down (usually some logarithmic terms appear) and hence one cannot use a differential model that would employ the corresponding derivatives.

We will show now how the problem (10)–(12) leads to a nice algebra of these poles. Consider the Fourier transform $\hat{v}_m(\xi, \varphi)$ of the function $v_m(\rho, \varphi)$ with respect to $\rho$ (i.e., the Mellin transform of the original function $V_m$):

$$\hat{v}_m(\xi, \varphi) = \frac{1}{\sqrt{2\pi}} \int_{-\infty}^{\infty} v_m(\rho, \varphi) e^{-i\rho\xi} \, d\rho. \tag{18}$$

Then equation (10) reduces to

$$-\xi^2 \hat{v}_m(\xi, \varphi) + \frac{\partial^2}{\partial\varphi^2} \hat{v}_m(\xi, \varphi) = 0 \tag{19}$$

with the boundary conditions

$$\hat{v}_m\left(\xi,\frac{\Phi}{2}\right)\mathrm{e}^{-\mathrm{i}m\Phi/2}=\hat{v}_m\left(\xi,-\frac{\Phi}{2}\right)\mathrm{e}^{\mathrm{i}m\Phi/2}=\widehat{w}_m(\xi),\tag{20}$$

$$\begin{aligned}&\mathrm{e}^{-\mathrm{i}m\Phi/2}\frac{\partial\hat{v}_m}{\partial\varphi}\left(\xi,\frac{\Phi}{2}\right)-\mathrm{e}^{\mathrm{i}m\Phi/2}\frac{\partial\hat{v}_m}{\partial\varphi}\left(\xi,-\frac{\Phi}{2}\right)\\&\quad=\lambda\frac{1}{\sqrt{2\pi}}\int_{-\infty}^{\infty}w_m(\rho)\Theta(\ln R-\rho)\mathrm{e}^{-\mathrm{i}\rho(\xi+\mathrm{i})}\,\mathrm{d}\rho.\end{aligned}\tag{21}$$

The solution of the Dirichlet boundary value problem (19)–(20) can be written as

$$\hat{v}_m(\xi,\varphi)=\widehat{w}_m(\xi)\left(\cos\left(\frac{m\Phi}{2}\right)\frac{\cosh\xi\varphi}{\cosh(\xi\Phi/2)}+\mathrm{i}\sin\left(\frac{m\Phi}{2}\right)\frac{\sinh\xi\varphi}{\sinh(\xi\Phi/2}\right).\tag{22}$$

Substituting this expression into the jump condition (21), we obtain an equation for $\widehat{w}(\xi)$:

$$\widehat{w}_m(\xi)\xi\frac{\cos m\Phi-\cosh\xi\Phi}{\sinh\xi\Phi}=\frac{\lambda}{2}\frac{1}{\sqrt{2\pi}}\int_{-\infty}^{\infty}w_m(\rho)\Theta(\ln R-\rho)\mathrm{e}^{-\mathrm{i}\rho(\xi+\mathrm{i})}\,\mathrm{d}\rho.\tag{23}$$

Using (16), this can be re-written as

$$\widehat{w}_{m,0}(\xi)=-\widehat{w}_{m,1}(\xi)+\frac{\lambda}{2}d_m(\xi)\big[\widehat{w}_{m,0}(\xi+\mathrm{i})+\big(w_{m,1}(\rho)\Theta(\ln R-\rho)\big)(\xi+\mathrm{i})\big],\tag{24}$$

where

$$d_m(\xi)=\frac{\sinh\xi\Phi}{\xi(\cos m\Phi-\cosh\xi\Phi)}=\frac{\mathrm{i}\sin(2\mathrm{i}\xi\pi/N)}{2\xi\sin((m-\mathrm{i}\xi)\pi/N)\sin((m+\mathrm{i}\xi)\pi/N)}.\tag{25}$$

Let us investigate the poles of $\widehat{w}_{m,0}(\xi)$ at the points $-\mathrm{i}n,\ n\in\mathbb{N}$. The equation (24) contains the shift by i in $\widehat{w}_{m,0}(\xi)$. Therefore, if one is aware of the behavior of $\widehat{w}_{m,0}(\xi)$ at 0 (and we are), then in order to decide how it behaves at $-\mathrm{i}n$, one needs to investigate the poles and zeros of $d_m(\xi)$. The following easily established statement collects the necessary (and even a little bit redundant) information about those.

**Lemma 1.**

1. All poles and zeros of $d_m(\xi)$ are located on the imaginary axis, and their location is $\mathrm{i}N$-periodic. In particular, one can study zeros and poles on the segment $(0\mathrm{i},-N\mathrm{i}]$ only.
2. All possible zeros of $d_m(\xi)$ on $(0\mathrm{i},-N\mathrm{i}]$ are located at the points $\xi=-\mathrm{i}N/2$ and $\xi=-\mathrm{i}N$.
3. All possible poles of $d_m(\xi)$ on $(0\mathrm{i},-N\mathrm{i}]$ are located at the points $\xi=-\mathrm{i}m$ and $\xi=-\mathrm{i}(N-m)$.

4. All points $\xi \in (0\mathrm{i}, -N\mathrm{i})$ except the ones listed above are regular with values

$$\frac{\sin n\Phi}{n(\cos m\Phi - \cos n\Phi)} \quad \text{at } \xi = -\mathrm{i}n.$$

5. If $N$ is even and $m = 0$, then $d_m(\xi)$ has a simple zero at $\xi = -\mathrm{i}N/2$ and a simple pole with the residue $(-\mathrm{i}/\pi)$ at $\xi = -\mathrm{i}N$. Other points $\xi \in (0\mathrm{i}, -N\mathrm{i})$ are regular with values $n^{-1}\cot(n\pi/N)$ at $\xi = -\mathrm{i}n$ for any $n \in (0, N)$, $n \neq N/2$.

6. If $N$ is even and $0 < m < N/2$, then $d_m(\xi)$ has a simple zero at $\xi = -\mathrm{i}N/2$ and simple poles at $\xi = -\mathrm{i}m$ and $\xi = -\mathrm{i}(N-m)$ with the residues $(-\mathrm{i}/m\Phi) = -\mathrm{i}N/(2\pi m)$ and $(-\mathrm{i}/(N-m)\Phi) = -\mathrm{i}N/(2\pi(N-m))$, respectively.

7. If $N$ is even and $m = N/2$, then $d_m(\xi)$ has a simple zero at $\xi = -\mathrm{i}N$ and a simple pole with the residue $2\mathrm{i}/\pi$ at $\xi = -\mathrm{i}N/2$.

8. If $N$ is odd and $m = 0$, then $d_m(\xi)$ has a simple pole with the residue $(-\mathrm{i}/\pi)$ at $\xi = -\mathrm{i}N$.

9. If $N$ is odd and $0 < m \leqslant [N/2]$, then $d_m(\xi)$ has simple poles at $\xi = -\mathrm{i}m$ and $\xi = -\mathrm{i}(N-m)$ with the residues $(-\mathrm{i}/m\Phi) = -\mathrm{i}N/(2\pi m)$ and $(-\mathrm{i}/(N-m)\Phi) = -\mathrm{i}N/(2\pi(N-m))$ respectively and a simple zero at $\xi = -\mathrm{i}N$.

Let us now start drawing some conclusions from (24). The last term in the square brackets in the right hand side of (24) is the Fourier transform of a compactly supported function, and therefore is an entire function of $\xi$. Since we assumed that $V_m(r,\varphi) < C/(1+r^\gamma)$ and hence $w_m(\rho) < C\mathrm{e}^{-\gamma\rho}$, function $\widehat{w}_{m,1}(\xi)$ is analytic in the complex half-plane $\operatorname{Im}\xi < \gamma$. Thus, we can write (24) as

$$\widehat{w}_{m,0}(\xi) = \frac{\lambda}{2} d(\xi)\widehat{w}_{m,0}(\xi + \mathrm{i}) + d(\xi) f_0(\xi) + f_1(\xi), \tag{26}$$

where the function $f_0(\xi)$ is entire, and $f_1(\xi)$ is analytic in the half-plane $\operatorname{Im}\xi < \gamma$. The assumed boundedness of the solution $w_m$ and (14) for $l = 0$ yield analyticity of $\widehat{w}_{m,0}(\xi)$ in the half-plane $\operatorname{Im}\xi > -\alpha$, except a pole at the origin:

$$\widehat{w}_{m,0}(\xi) = \frac{\mathrm{i}v_{m,0}}{\sqrt{2\pi}\xi} + h_1(\xi), \quad \operatorname{Im}\xi > -\alpha, \tag{27}$$

where $h_1(\xi)$ is a function analytic for $\operatorname{Im}\xi > -\alpha$. Now equation (26), used repeatedly, implies analyticity of $\widehat{w}_{m,0}(\xi)$ in the whole plane except for the points $\xi = -\mathrm{i}n$, $n = 0, 1, 2, \ldots,$ where this function can have poles. These poles, as we have already pointed out before, determine behavior of $w_m(r)$ near the origin, which is our current object of interest.

We will now address separately the cases of even and odd values of $N$.

*3.2. Even N*

We are interested in the possibility of the expansion (17)

$$\widehat{w}_{m,0}(\xi) = \frac{\mathrm{i}}{\sqrt{2\pi}} \sum_{n=0}^{l} \frac{v_{m,n}}{\xi + \mathrm{i}n} + A(\xi), \tag{28}$$

and if it exists, in its coefficients. Let

$$\widehat{w}_{m,0}(-\mathrm{i}n + \eta) = \sum_{j=-\infty}^{\infty} S_{m,n}^{(j)} \frac{1}{\eta^j} \tag{29}$$

be the Laurent expansion of $\widehat{w}_{m,0}(\xi)$ near the point $-\mathrm{i}n$. Assuming (17), we see that for $n \leqslant l$ we must have $S_{m,n}^{(j)} = 0$ for $j \geqslant 2$ and $S_{m,n}^{(1)} = \mathrm{i}v_{m,n}/\sqrt{2\pi}$. So, knowledge of (29) would provide the needed information about (17).

Consider first the case when $m = 0$.

According to (27), the highest term in the Laurent expansion near 0 corresponds to a simple pole:

$$S_{0,0}^{(1)} = \frac{\mathrm{i}v_{0,0}}{\sqrt{2\pi}}. \tag{30}$$

For $n = 1, \ldots, N/2 - 1$ function $d(\xi)$ has no zeros or poles at the points $\xi = -\mathrm{i}n$, so equation (26) jointly with the lemma tell that

$$v_{0,n} = \frac{(-\lambda)^n}{n! 2^n} \left( \prod_{j=1}^{n} \cot \frac{\Phi}{2} \right) v_{0,0}. \tag{31}$$

When $n$ reaches the value $N/2$, function $d(\xi)$ has a simple zero, which according to (26) means cancellation of the pole. Hence, $\widehat{w}_0(\xi)$ is analytic at $-\mathrm{i}N/2$ and $S_{0,N/2}^{(1)} = 0$. Since according to the lemma $d(\xi)$ does not have any poles for $\xi = -\mathrm{i}n,\ n = N/2 + 1, \ldots, N - 1$, we conclude that $v_{0,n} = S_{0,n}^{(1)} = 0$ for $n \in [N/2, N)$.

When $n = N$, function $d(\xi)$ has a simple pole, which produces a new singularity

$$S_{0,N}^{(1)} = \frac{C}{\eta}, \tag{32}$$

where the value of the constant $C$ can be found from (24). If $C$ is not equal to zero, the above calculation should be repeated again, and so on, since the trigonometric part of the expression defining $d(\xi)$ is periodic with period $2N\mathrm{i}$.

Consider now the case when $0 < m < N/2$.

When $m \neq 0$, continuity of the solution at the vertex together with condition (8) imply that

$$v_{m,0} = V_m\left(0, \frac{\Phi}{2}\right) = V_m\left(0, -\frac{\Phi}{2}\right) = 0. \tag{33}$$

According to the lemma, this means then that for $n = 0, \dots, m-1$ there are no singularities at $\xi = -\mathrm{i}n$, i.e., $v_{m,n} = S^{(1)}_{m,n} = 0$. When $n = m$, a simple pole can arise with a residue $S^{(1)}_{m,m} = \mathrm{i}v_{m,m}/\sqrt{2\pi}$. This pole then "propagates" while $n < N/2$:

$$v_{m,n} = \frac{(-\lambda)^{n-m}}{(n-m)!2^{n-m}}\left(\prod_{j=m+1}^{n}\frac{\sin j\Phi}{\cos m\Phi - \cos j\Phi}\right)v_{m,m}. \tag{34}$$

When $n$ becomes equal $N/2$, the singularity gets cancelled by a zero of $d(\xi)$, and $\widehat{w}_0(\xi)$ stays analytic for $\xi = -\mathrm{i}n,\ n = N/2, \dots, N-m-1$. At the point $n = N-m$ a simple pole is generated by the pole of $d(\xi)$. It then survives for $n = N-m, \dots, N-1$, and get canceled by a zero of $d(\xi)$ at $n = N$.

Consider now the last case $m = N/2$.

As before, since $m \neq 0$, we have $v_{N/2,0} = 0$. Hence, for $n = 0, \dots, N/2-1$ there are no singularities at $\xi = -\mathrm{i}n$ and thus $v_{N/2,n} = S^{(1)}_{N/2,n} = 0$. When $n = N/2$, a simple pole can arise with a residue $v_{N/2,N/2} = S^{(1)}_{N/2,N/2}$. This pole "propagates" till $n = N$, where it gets cancelled by a zero of $d(\xi)$.

The above consideration shows that all singularities in the case of even $N$ are at most simple poles. Hence, $\widehat{w}_{m,0}(\xi)$ is a meromorphic function with simple poles at $\xi = -\mathrm{i}n,\ n = 0, 1, 2, \dots,$ with the residues $S^{(1)}_{m,n}$. Since the fraction $1/(\xi + \mathrm{i}n)^j$ corresponds under the Fourier transform to the function

$$\begin{cases} \dfrac{-\mathrm{i}^j\sqrt{2\pi}\,\rho^{j-1}\mathrm{e}^{n\rho}}{(j-1)!}, & \rho \leqslant 0, \\ 0, & \rho > 0, \end{cases} \tag{35}$$

$w_m(\rho)$ can be represented for $\rho \to -\infty$ by the asymptotic series

$$w_m(\rho) \sim \sum_{n=0}^{\infty} v_{m,n}\mathrm{e}^{n\rho}, \tag{36}$$

where $v_{m,n} = -\mathrm{i}\sqrt{2\pi}\,S^{(1)}_{m,n}$, and, according to (22),

$$V_m(r,\varphi) \sim \sum_{n=0}^{\infty} r^n(a_{m,n}\cos n\varphi + b_{m,n}\sin n\varphi), \tag{37}$$

where $-\Phi/2 < \varphi < \Phi/2$, and coefficients $a_{m,n}$ and $b_{m,n}$ can be easily expressed in terms of $v_{m,n}$. It is interesting to notice that $a_{m,n} = b_{m,n} = 0$ for $n < m$:

$$V_m(r,\varphi) \sim \sum_{n=m}^{\infty} r^n(a_{m,n}\cos n\varphi + b_{m,n}\sin n\varphi). \tag{38}$$

It follows then from the jump condition (9), that the first term of the expansion (37) can be written on each of $N$ angular domains between the edges of the star structure as a single function, i.e.,

$$V_m(r,\varphi) = r^m(a_{m,m}\cos m\varphi + b_{m,m}\sin m\varphi) + \mathrm{o}\big(r^m\big), \quad 0 \leqslant \varphi \leqslant 2\pi. \tag{39}$$

### 3.3. Odd N

Consider first the case when $m = 0$. Like before, the highest term in the Laurent expansion of $\widehat{w}_{m,0}(\xi)$ near 0 corresponds to a simple pole:

$$S^{(1)}_{0,0} = \frac{\mathrm{i}v_{0,0}}{\sqrt{2\pi}}. \tag{40}$$

For $n = 1, \dots, N-1$ we do not hit either zeros or poles of $d(\xi)$, and hence the simple pole survives at these points with the residue $S^{(1)}_{0,n} = \mathrm{i}v_{0,n}/\sqrt{2\pi}$,

$$v_{0,n} = \frac{(-\lambda)^n}{n!2^n}\left(\prod_{j=1}^{n}\cot\frac{\Phi}{2}\right)v_{0,0}. \tag{41}$$

When $n = N$, the pole of $d(\xi)$ introduces a second order pole of $\widehat{w}_{m,0}(\xi)$ with the coefficient

$$S^{(2)}_{0,N} = \frac{2\mathrm{i}}{n\Phi}S^{(1)}_{0,N-1}. \tag{42}$$

Generally, coefficient $S^{(1)}_{0,N}$ is not equal to zero; hence, the term $S^{(1)}_{0,N}/(\xi + \mathrm{i}N)$ can also be present in the Laurent expansion of $\widehat{w}_{m,0}(\xi)$ near $-\mathrm{i}N$.

For larger $n$ this situation will repeat periodically with the period $N$, i.e., each time when $n = kN$ the order of the highest term will increase by one.

Consider now case $0 < m \leqslant [N/2]$.

As it has been already mentioned before, when $m \neq 0$, the coefficients $v_{m,0}$ are equal to zero. Then, for $n = 0, \dots, m-1$ there are no singularities at $\xi = -\mathrm{i}n$, i.e., $v_{m,n} = S^{(1)}_{m,n} = 0$. When $n = m$, a simple pole can arise with a residue $S^{(1)}_{m,m}$. This pole then propagates while $n < N - m$:

$$v_{m,n} = \frac{(-\lambda)^{n-m}}{(n-m)!2^{n-m}}\left(\prod_{j=m+1}^{n}\frac{\sin j\Phi}{\cos m\Phi - \cos j\Phi}\right)v_{m,m}. \tag{43}$$

When $n$ becomes equal to $N - m$, we obtain a second order pole with

$$S^{(2)}_{0,N-m} = -\frac{\mathrm{i}}{n\Phi}S^{(1)}_{0,N-m-1}. \tag{44}$$

The residue at this point can be also nonzero. This second order pole then propagates while $n < N$:

$$S_{0,n}^{(2)} = S_{0,N-m}^{(2)} \prod_{j=N-m+1}^{n} \frac{-(\lambda/2)\sin j\Phi}{j(\cos m\Phi - \cos j\Phi)}, \quad N - m < n < N. \tag{45}$$

When $n = N$, the order of the highest term increases by one, and this goes on periodically with period $N$.

Formula (35) for the inverse Fourier transforms of poles $1/(\xi + \mathrm{i}n)^j$ leads to the following expansion for $V_m(r, \varphi)$:

$$V_m(r, \varphi) = \sum_{n=m}^{L_m} r^n (a_{m,n} \cos n\varphi + b_{m,n} \sin n\varphi) + \mathrm{o}\big(r^{L_m}\big), \tag{46}$$

where $L_m = N - m - 1$ for $m > 0$ and $L_0 = N - 1$. Like for even $N$, the first $m - 1$ harmonics are absent in the expansion of $V_m(r, \varphi)$. The remainder of the expansion (46) contains terms of the form $r^k \log^l(r) f_{k,l}(\varphi)$. The minimal number of the terms that are differentiable at the origin is equal to $[N/2]$; this occurs when $m = [N/2]$.

### *3.4. Construction of the differential operators on graphs*

The above consideration suggests the order of the differential operator (4) and boundary conditions to be used to approximate the high-frequency asymptotics of the Dirichlet-to-Neumann operator $\Lambda_\Sigma$ on the graph $\Sigma$.

In order to pose boundary conditions for the differential operator $A_M$, we assume that all nodes of the graph are symmetric junctions of $N$ edges. In order to figure out the boundary conditions at the symmetric junctions, we use relations (38) and (46) that describe behavior of the Dirichlet-to-Neumann eigenmodes near the vertex of the $N$ point star structure.

As the above analysis shows, the number of differentiable terms in (38) and (46) for which the coefficients can be determined from (26) (and hence from the spectral problem for $\Lambda_\Sigma$) for all $m$ such that $|m| \leqslant [N/2]$ is limited by $[N/2]$ for both even and odd $N$. Hence, it seems unreasonable to try to impose conditions on derivatives of order higher than $[N/2]$, since some of the eigenmodes might not possess those. On the other hand, expansions (38) and (46) for certain values of $m$ contain terms with the first $[N/2] - 1$ derivatives equal to zero at the origin. Therefore, conditions on at least $[N/2]$ first derivatives should probably be posed. Since these conditions have to be posed on both ends of the graph edges, the order of the operator should be equal to $2[N/2]$, i.e., constant $M$ in the definition (4) of the operator $A_M$ should be equal $[N/2]$. This implies in particular that while in the case of a triple junction ($N = 3$) one can try to use a second order differential problem on $\Sigma$, for the square structure ($N = 4$) only the fourth order ODEs should be employed. Although we will consider the case $N = 4$ in detail in a forthcoming paper, we can mention that numerics does confirm that $M = 1$ is unsuitable for $N = 4$, while $M = 2$ does work.

We define boundary conditions at the nodes as follows. According to the expansions (38) and (46) and condition (7), restriction $u_{m,j}(r)$ of the eigenmode $V_m(r,\varphi)$ to the $j$th edge is equal to

$$u_{m,j}(r) = w_m(r)\mathrm{e}^{-\mathrm{i}m\Phi/2}\mathrm{e}^{\mathrm{i}jm\Phi} = \mathrm{e}^{\mathrm{i}jm\Phi}\sum_{n=m}^{[N/2]} v_{m,n}r^n + \mathrm{o}\big(r^{[N/2]}\big). \tag{47}$$

Hence, one expects the most general form of the solution of the differential equation at the junction to be

$$u_j(r) \sim \sum_{m=-[N/2]}^{[N/2]} C_m u_{m,j}(r) = \sum_{m=-[N/2]}^{[N/2]} C_m \mathrm{e}^{\mathrm{i}jm\Phi}\sum_{n=|m|}^{[N/2]} v_{|m|,n}r^n. \tag{48}$$

This together with our study of the coefficients $v_{m,n} = -\mathrm{i}\sqrt{2\pi}S^{(1)}_{m,n}$ leads to some linear relations among the derivatives $v_j^{(l)}(0)$. Knowing these, one can attempt for particular geometries to write down and study the corresponding spectral ODE problem on the graph $\Sigma$. Since this becomes kind of technical, we will do it in a separate section below.

## 4. Examples of spectral calculations

In this section we will use the results of the considerations above in order to define and study the appropriate spectral problem for an operator $A_M$. We will see, in particular, that this problem must also contain the spectral parameter in the boundary conditions. Then the resulting spectra will be compared with the pseudo-differential ones computed numerically.

### 4.1. Structures with symmetric triple junctions

Consider a structure that has symmetric triple junctions only (i.e., at each vertex three edges meet at the 120° angles). Then expansion (48) together with formulas (41) and (43) yields the following boundary conditions at a junction:

$$u_j(r) = v_{-1,1}\mathrm{e}^{-\mathrm{i}j\Phi}r + v_{0,0}\left(1 - r\frac{\lambda}{2}\cot\frac{\pi}{3}\right) + v_{1,1}\mathrm{e}^{\mathrm{i}j\Phi}r + \mathrm{o}(r). \tag{49}$$

Describing arbitrary linear behavior along three edges requires six coefficients $v_{m,n}$ ($m = -1, 0, 1,\ n = 0, 1$). However, the representation (49) contains three parameters only. Thus, three linear conditions must be satisfied by the values $u_j(0)$ and $u_j'(0)$. It is not hard to see that (49) is equivalent to the following vertex conditions:

$$\begin{cases} u_1(0) = u_2(0) = u_3(0), \\ \displaystyle\sum_{j=1}^{3} \frac{\mathrm{d}u_j}{\mathrm{d}r}(0) = -\lambda\frac{3u_1(0)}{2}\cot\frac{\pi}{3}. \end{cases} \tag{50}$$

Indeed, the first set of conditions implies that $v_{j,0} = 0$ for $j \neq 0$. The second means that if one considers the function $(\mathrm{d}u_j/\mathrm{d}r)(0)$ on the group $\mathbb{Z}_3$, its Fourier expansion starts with the constant term equal to $-v_{0,0}(\lambda/2)\cot(\pi/3)$. This is obviously equivalent to (49). The $r$-derivatives above are computed in the direction from the node towards the middle of the edge.

Let us specify this for certain geometries of $\Sigma$.

*4.1.1. Honeycomb structure*

In this section we calculate the spectrum of the differential problem (5) with boundary conditions (50) for the honeycomb structure (figure 3).

The fundamental cell for this structure is shown in figure 4. Here $L$ denotes the length of each edge.

Since the whole structure is periodic, one needs to use the Floquet–Bloch theory (see, for instance, [2,19,49,50,59] and impose cyclic conditions on the boundaries of the cell with a quasimomentum $k = (k_1, k_2)$. This means that the vertical shift by $\sqrt{3}L$ results in multiplication of a function by $\mathrm{e}^{\mathrm{i}k_1}$, while the horizontal shift by $3L$ reduces to multiplication by $\mathrm{e}^{\mathrm{i}k_2}$. This is reflected on figure 4, where it is shown that shift "North" by the period is equivalent to multiplication by $\mathrm{e}^{\mathrm{i}k_1}$ and shift "East" multiplies by $\mathrm{e}^{\mathrm{i}k_2}$. In particular, only four vertices $A$, $B$, $C$, and $D$ in the unit cell are required. Then the resulting spectrum $\lambda_l(k)$ as a function of $k$ is the so called dispersion relation (or dispersion curve, or band function). It is well known (see the quotes above) that the spectrum in the whole plane coincides with the union over $k$ of these spectra (i.e., with the range of the band function).

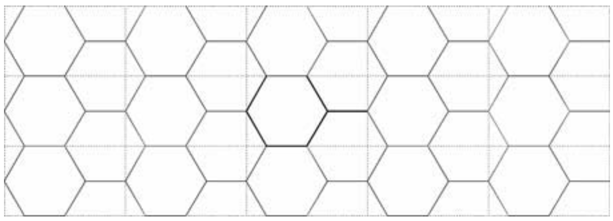

Figure 3. Honeycomb structure.

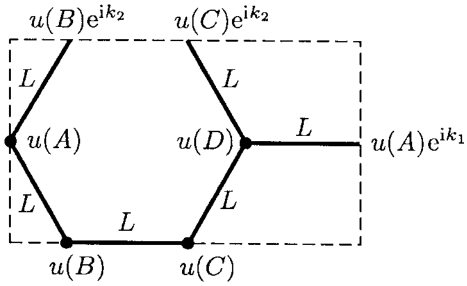


Figure 4. The fundamental cell of the honeycomb structure.

The whole problem on the honeycomb graph $\Sigma$ now reduces to the following system on the union of six edges in the unit cell:

$$\begin{cases} \dfrac{\mathrm{d}^2}{\mathrm{d}l^2}u(l) = -\left(\dfrac{\lambda}{2}\right)^2 u(l) & \text{on each edge,} \\ u_1(0) = u_2(0) = u_3(0) & \text{at each vertex,} \\ \displaystyle\sum_{j=1}^{3} \frac{\mathrm{d}u_j}{\mathrm{d}r}(0) = -\lambda \frac{3u_1(0)}{2} \cot\frac{\pi}{3} & \text{at each vertex,} \\ u(x+3L, y) = \mathrm{e}^{\mathrm{i}k_2} u(x,y), \\ u(x, y+\sqrt{3}L) = \mathrm{e}^{\mathrm{i}k_1} u(x,y), \end{cases} \tag{51}$$

where $x$ is the horizontal and $y$ is the vertical coordinate.

Surprisingly enough, the spectrum of (51) can be explicitly described.

**Theorem 2.** The dispersion curves $\lambda(k)$ for (51) consist of the constant branches $\lambda_m = 2\pi m/L,\ m \in \mathbb{N}$, and of the graphs of the functions

$$\lambda_n(k) = \frac{2}{L}\left(\pi n + \frac{\pi}{3} \pm \arcsin\sqrt{\frac{1}{4} + \frac{1}{6}\cos k_2 \pm \frac{1}{6}\sqrt{(1+\cos k_1)(1+\cos k_2)}}\right), \tag{52}$$

where $n \in \mathbb{N}$. In particular, the spectrum of the ODE on the periodic graph $\Sigma$ is the union of segments $[2\pi n/L, (4\pi/3 + 2\pi n)/L]$ for $n \in \mathbb{N}$.

*Proof.* There are six edges inside the unit cell. Solution of the second-order differential equation in (51) on each edge can be represented as

$$u_j(r) = c_{1,j}\cos\left(\frac{\lambda r}{2}\right) + c_{2,j}\sin\left(\frac{\lambda r}{2}\right). \tag{53}$$

Hence, we have twelve unknown coefficients to determine and twelve equations given by conditions (50) at each of the four nodes $A,\ B,\ C$, and $D$. Eight of these twelve equations are continuity conditions, while the other four relate derivatives to the values of the solution at the nodes.

Let us notice first the following interesting feature. When the value of the spectral parameter $\lambda$ is equal to $2\pi n/L,\ n \in \mathbb{N}$, one can choose all coefficients $c_{1,j}$ to be equal to zero. Then the solution $u_j(r) = c_{2,j}\sin(\lambda r/2)$ vanishes at the nodes (i.e., $u_i(0) = u_i(L) = 0$). Therefore, all eight continuity conditions are satisfied. Since now the function is equal to zero at the nodes, the other four conditions (50) are equivalent to the sum of the derivatives at each node being equal to zero. These four linear equations can always (for any quasimomentum $k$) be satisfied by choosing properly six constants $c_{2,i}$, some of which can be chosen not to equal zero. Hence, for $\lambda_n = 2\pi n/L$ the problem (51) has a nonzero solution for any quasimomentum $k$. This means that these values of $\lambda$ are eigenvalues of the problem for any $k$. In terms of the dispersion curves this means presence of flat branches on these levels. Their existence is known to correspond to presence of the so called bound states (see, for instance, [2,49,50,59]),

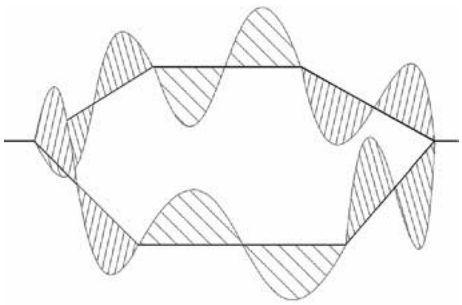

Figure 5. A compactly supported eigenfunction.

i.e., to existence of square-integrable eigenfunctions of the problem considered on the infinite periodic graph. This is considered to normally be an impossibility for periodic media [2,19,49,50,59]. However, as, in particular, our observation shows, differential problems on periodic graphs, due to a nontrivial topology can possess bound states in some resonant situations (see also [7,50,51]). In our case it is easy to even construct compactly supported eigenfunctions corresponding to the above eigenvalues. Consider, for example, the sinusoidal wave defined by the formula $u_i(r) = c_{2,i} \sin(2\pi r/L)$, where $|c_{2,i}| = 1$ on one of the hexagonal loops of the honeycomb structures and equal to zero on the rest of the infinite graph (figure 5).

This solution vanishes at the nodes of the graph and the sum of the derivatives at each of the nodes is equal to zero. Existence of eigenvalues of differential operators on periodic graphs seems to be a new spectral effect overlooked before in the context of mesoscopic physics.

Let us now consider the bulk of the spectrum. If the spectral parameter $\lambda$ is not equal to $2\pi m/L$, constants $c_{1,j}$ and $c_{2,j}$ can be expressed (using (53) and continuity condition at the nodes) in terms of the four node values $u(A)$, $u(B)$, $u(C)$, and $u(D)$ (see figure 4). Conditions (50) for the derivatives at these nodes lead to the following homogeneous system of equations:

$$\begin{cases} f(\lambda)u(A) + \left(e^{ik_2}+1\right)u(B) + e^{-ik_1}u(D) = 0, \\ \left(e^{-ik_2}+1\right)u(A) + f(\lambda)u(B) + u(C) = 0, \\ u(B) + f(\lambda)u(C) + \left(e^{-ik_2}+1\right)u(D) = 0, \\ e^{ik_1}u(A) + \left(e^{ik_2}+1\right)u(C) + f(\lambda)u(D) = 0, \end{cases} \tag{54}$$

where $f(\lambda) = 2\sqrt{3}\sin(\lambda L/2 - \pi/3)$. The determinant of this system is equal to

$$\begin{vmatrix} f(\lambda) & e^{ik_2}+1 & 0 & e^{-ik_1} \\ e^{-ik_2}+1 & f(\lambda) & 1 & 0 \\ 0 & 1 & f(\lambda) & e^{-ik_2}+1 \\ e^{ik_1} & 0 & e^{ik_2}+1 & f(\lambda) \end{vmatrix} \tag{55}$$

$$= f^4(\lambda) - 2\left(g(k_2)+1\right)f^2(\lambda) + g^2(k_2) - 2g(k_2)\cos k_1 + 1, \tag{56}$$

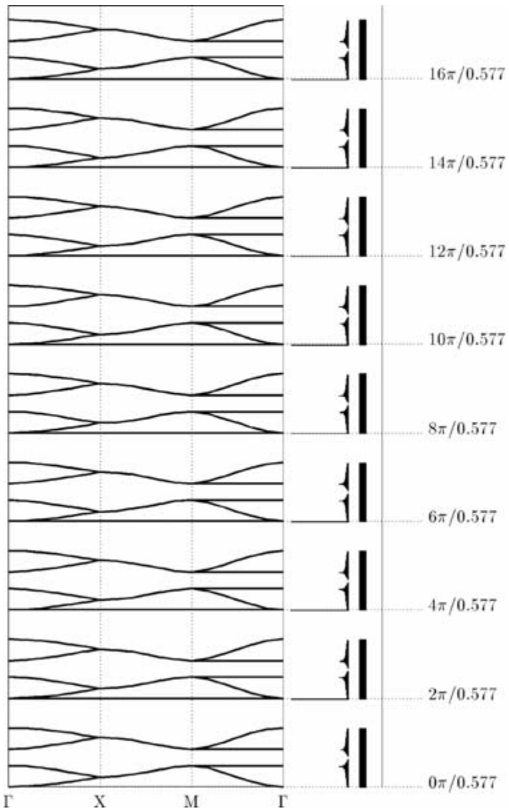


Figure 6. The spectrum of the differential problem (51) on the honeycomb structure.

where $g(k) = 2 + 2\cos k$. The system has a nontrivial solution iff its determinant is equal to zero, which leads to

$$f^2(\lambda) = g(k_2) + 1 \pm \sqrt{g(k_1)g(k_2)}. \tag{57}$$

One can solve this equation for $\lambda$ and obtain analytic expression for the dispersion relation:

$$\lambda_n(k) = \frac{2}{L}\left(\pi n + \frac{\pi}{3} \pm \arcsin\sqrt{\frac{1}{4} + \frac{1}{6}\cos k_2 \pm \frac{1}{6}\sqrt{(1+\cos k_1)(1+\cos k_2)}}\right). \tag{58}$$

Analyzing (57), one can see that as the quasimomentum $k$ varies over Brillouin zone $[0,\pi] \times [0,\pi]$, function $f^2(\lambda)$ covers the interval $[0, 9]$, which is equivalent to the spectral parameter $\lambda$ covering intervals $[2\pi n/L, (4\pi/3 + 2\pi n)/L]$. Thus the union of these intervals represents the spectrum of the problem. This finishes the proof of the theorem. $\square$

The spectrum is shown in figure 6 along with the dispersion relations for $L = 1/\sqrt{3} \cong 0.5773$.

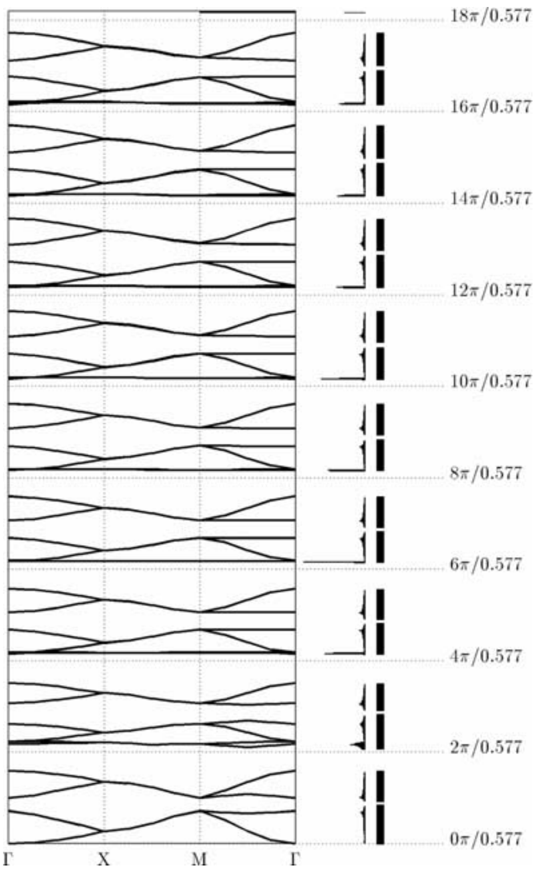


Figure 7. The spectrum of the operator $\Lambda_\Sigma$ on the honeycomb structure.

It is interesting to compare this spectrum with the dispersion curves and the spectrum of the pseudodifferential operator $\Lambda_\Sigma$ computed numerically by the method of [51] (shown in figure 7).

The two spectra are practically identical starting with the second spectral band (and very close for the first one). This amazing agreement shows validity of our heuristic approach.

We would like to mention the following interesting feature of these two graphs that in spite of their similarity sets them apart. Both of them appear to show the phenomenon of flat bands at the levels $\lambda_m = 2\pi m/L$. One can notice, however, that the lower of these bands in the pseudo-differential case look not exactly constant. This is not an accident. Although in the differential case, as we have shown, these bands are exactly flat, and hence correspond to actual bound states, we have conjectured before [50,51] that the spectrum of $\Lambda_\Sigma$ is absolutely continuous, so in the pseudo-differential case these bands are not exactly constant. This conjecture was proven in [8]. This means that in the case of $\Lambda_\Sigma$ one deals with strong resonances rather than actual bound states.

*4.1.2. Quasi-octagonal structure*

In this section we will compute the spectrum of the following quasi-octagonal structure shown in figure 8.

The graph $\Sigma$ consists of straight edges and arcs of the same length $L$. Like the previous structure, this one contains only symmetric triple junctions. If all the edges of octagons and squares were straight, the junctions would not be symmetric, so the sides of the "squares" have been made curved in order to preserve the symmetry of the junction. This explains the name we gave to this geometry.

We construct again the ODE spectral problem on $\Sigma$ as follows:

$$\begin{cases} \dfrac{\mathrm{d}^2}{\mathrm{d}l^2}u(l) = -\left(\dfrac{\lambda}{2}\right)^2 u(l) & \text{on each edge,} \\ u_1(0) = u_2(0) = u_3(0) & \text{at each vertex,} \\ \displaystyle\sum_{j=1}^{3} \dfrac{\mathrm{d}u_j}{\mathrm{d}r}(0) = -\lambda \dfrac{3u_1(0)}{2} \cot \dfrac{\pi}{3} & \text{at each vertex.} \end{cases} \tag{59}$$

The spectrum and dispersion curves for this problem can be studied explicitly.

**Theorem 3.** The dispersion curves for (59) consist of the flat branches $\lambda_m = 2\pi m/L$, $m \in \mathbb{N}$ and of the branches given by the equation

$$f^4(\lambda) - 6f^2(\lambda) + 4f(\lambda)(\cos k_1 + \cos k_2) + 1 - 4\cos k_1 \cos k_2 = 0, \tag{60}$$

where $f(\lambda) = 2\sqrt{3}\sin(\lambda L/2 - \pi/3)$. In particular, the spectrum of (59) is the union of the segments $(2/L)[\pi m, \pi m + \frac{2}{3}\pi]$, $m \in \mathbb{N}$.

*Proof.* Like for the honeycomb structure, modulo the lattice of periods, there are six edges inside each unit cell. We impose, as before, the Floquet–Bloch cyclic conditions on the boundary of the cell with certain quasimomentum $k = (k_1, k_2)$. Solution of the second-order differential equation (5) on each edge can be represented by the formula (53). Hence, we have twelve unknown coefficients to determine and twelve equations given by conditions (50) at each of the four nodes $A, B, C$, and $D$. Eight of these twelve equations are continuity conditions, while the other four relate derivatives to the values of the solution at the nodes.

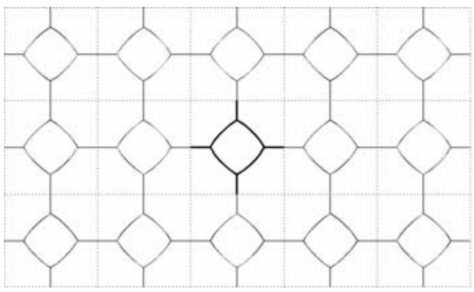

Figure 8. Quasi-octagonal structure.

Exactly like we did this for the honeycomb structure, we establish the presence of the flat branches $\lambda_m = 2\pi m/L$. So, one observes bound states again.

If $\lambda$ is not equal to $2\pi m/L$, constants $c_{1ji},\ c_{2,j}$ in (53) can be expressed using the values at the four nodes. The four conditions on derivatives at the nodes lead to the following homogeneous system of equations:

$$\begin{cases} f(\lambda)u(A) + u(B) + u(C)\mathrm{e}^{-\mathrm{i}k_2} + u(D) = 0, \\ u(A) + f(\lambda)u(B) + u(C) + u(D)\mathrm{e}^{-\mathrm{i}k_1} = 0, \\ u(A)\mathrm{e}^{\mathrm{i}k_2} + u(B) + f(\lambda)u(C) + u(D)\mathrm{e}^{-\mathrm{i}(k_2-k_1)} = 0, \\ u(A) + \mathrm{e}^{\mathrm{i}k_1}u(B) + \mathrm{e}^{\mathrm{i}(k_2-k_1)}u(C) + f(\lambda)u(D) = 0, \end{cases} \tag{61}$$

where as for the honeycomb geometry before $f(\lambda) = 2\sqrt{3}\sin(\lambda L/2 - \pi/3)$. The determinant of this system is

$$\begin{vmatrix} f(\lambda) & 1 & \mathrm{e}^{-\mathrm{i}k_2} & 1 \\ 1 & f(\lambda) & 1 & \mathrm{e}^{-\mathrm{i}k_1} \\ \mathrm{e}^{\mathrm{i}k_2} & 1 & f(\lambda) & \mathrm{e}^{-\mathrm{i}(k_2-k_1)} \\ 1 & \mathrm{e}^{\mathrm{i}k_1} & \mathrm{e}^{\mathrm{i}(k_2-k_1)} & f(\lambda) \end{vmatrix} \tag{62}$$

$$= f^4(\lambda) - 6f^2(\lambda) + 4f(\lambda)(\cos k_1 + \cos k_2) + 1 - 4\cos k_1 \cos k_2. \tag{63}$$

The determinant is equal to zero iff the values of the polynomial (in $f$)

$$y = \frac{1}{4}\left(f^4 - 6f^2 + 1\right) \tag{64}$$

and of the linear function $Y_k$

$$y = \cos k_1 \cos k_2 - f(\cos k_1 + \cos k_2) \tag{65}$$

coincide at this particular value of $f$. One can readily check that for $k \in [0,\pi] \times [0,\pi]$ the set of lines $Y_k$ covers the shaded domain in figure 9, and the graph of the

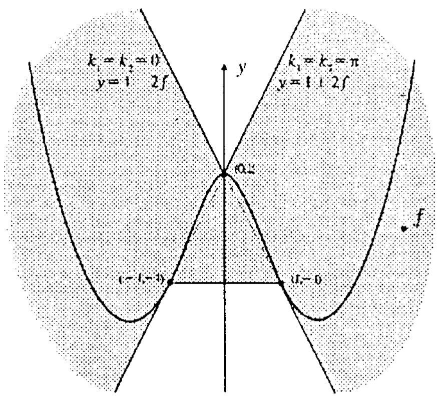


Figure 9. The graph of $y = (1/4)(f^4 - 6f^2 + 1)$ and the area covered by the set of lines $Y_k$.

polynomial belongs to this domain, touching its boundary at the points $(-1, -1)$, $(0, 1)$, and $(1, -1)$, until it escapes to infinity crossing the lines $y = 1 \pm 2f$.

Hence, solution exists for any $f$ between these "escape" intersections of the graph of $y = \frac{1}{4}(f^4 - 6f^2 + 1)$ with the lines $y = 1 + 2f$ and $y = 1 - 2f$. These lines correspond to the cases $k_1 = k_2 = \pi$ and $k_1 = k_2 = 0$ respectively. In these cases the equation for $f$

$$f^4 - 6f^2 + 4f(\cos k_1 + \cos k_2) + 1 - 4\cos k_1 \cos k_2 = 0 \tag{66}$$

has the sets of roots $\{3, -1, -1, -1\}$ and $\{-3, 1, 1, 1\}$, correspondingly. Therefore, the escape values of $f$ are $\pm 3$, and hence the spectrum covers intervals defined by the condition $-3 \leqslant f(\lambda) \leqslant 3$ or $\lambda L/2 \in [\pi k, \pi k + \frac{2}{3}\pi]$. This finishes the proof. $\square$

Figure 10 demonstrates the spectrum of the differential problem for $L = 0.418$ along with the numerically computed dispersion relations.

This spectrum closely approximates the numerically computed spectrum of the pseudodifferential operator $\Lambda_\Sigma$ (figure 11):

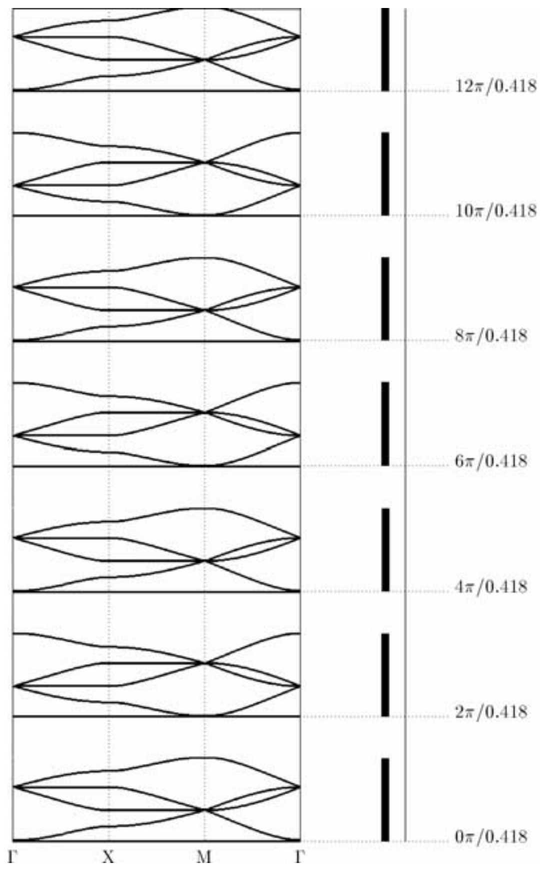


Figure 10. The spectrum of the differential problem on the quasi-octagonal structure.

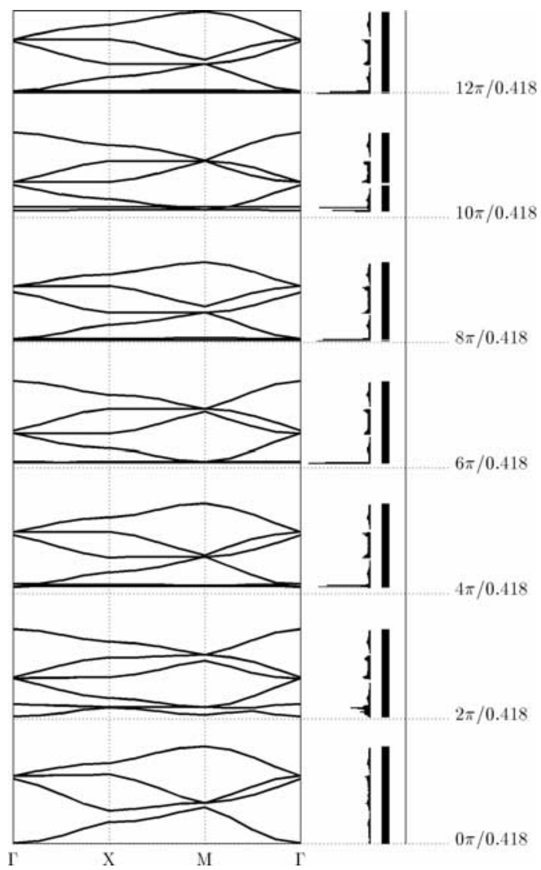


Figure 11. Disperison relations and the spectrum for $\Lambda_\Sigma$ on the quasi-octagonal structure.

Our remark (made with the reference to the honeycomb structure) concerning the difference between presence of bound states (differential problem) and resonances (pseudo-differential problem) and related to the result of [8], applies here too.

## 5. Final remarks and conclusions

In this paper we presented a partly rigorous, partly heuristic procedure for approximating spectra of pseudo-differential operators on graphs that arise in the photonic crystal theory by spectra of much simpler differential problems. The main advantage of considering differential problems is that their spectra are easy to study. In simplest cases it can be done analytically. In contrast, study of the original pseudo-differential problem and of spectra of photonic crystals in general requires not very simple numerics (see, for instance, [6,18,26]) and usually does not submit easily to analytic investigation.

Spectra of the constructed differential problems show an amazingly good agreement with the spectra of the original pseudodifferential problems. In the smooth case, i.e., when vertices are absent, the corresponding result was rigorously proven in our previous work [51] (see also [7,50] for surveys). Although the numeric evidence suggests strongly that approach works in a more general case considered here, it is not clear yet how to carry over our rigorous justification of the spectral approximation [51] from the smooth case to the case of a graph.

Due to space limitations, only the case of symmetric triple junction was considered in detail. We plan to address the quadruple junctions and free ends (square structures, crosses, etc.) elsewhere, where we will also consider some other spectral effects.

## Acknowledgements

This research was partly sponsored by the NSF through the Grants DMS 9610444 and DMS 0072248 and by the Army Research Office of the Department of Army and the State of Kansas through a DEPSCoR Grant. The authors thank the NSF, ARO, and the State of Kansas for this support. The content of this paper does not necessarily reflect the position or the policy of the federal government, and no official endorsement should be inferred.

The authors also express their gratitude to the reviewer for useful remarks.

## References

[1] S. Alexander, Superconductivity of networks. A percolation approach to the effects of disorder, Phys. Rev. B 27 (1983) 1541–1557.

[2] N.W. Ashcroft and N.D. Mermin, *Solid State Physics* (Holt, Rinehart and Winston, New York/London, 1976).

[3] A. Aviram and M. Ratner, eds., *Molecular Electronics: Science and Technology*, Ann. New York Acad. Sci., Vol. 852 (1998).

[4] Y. Avishai and J.M. Luck, Quantum percolation and ballistic conductance on a lattice of wires, Phys. Rev. B 45(3) (1992) 1074–1095.

[5] J.E. Avron, A. Raveh and B. Zur, Adiabatic quantum transport in multiply connected systems, Rev. Mod. Phys. 60(4) (1988) 873–915.

[6] W. Axmann and P. Kuchment, An efficient finite element method for computing spectra of photonic and acoustic band-gap materials I. Scalar case, J. Comput. Phys. 150 (1999).

[7] W. Axmann, P. Kuchment and L. Kunyansky, Asymptotic methods for thin high contrast 2D PBG materials, J. Lightwave Technology 17(11) (1999) 1996–2007.

[8] M.S. Birman, T.A. Suslina and R.G. Shterenberg, Absolute continuity of the spectrum of a two-dimensional Schrödinger operator with potential supported on a periodic system of curves, Preprint ESI No. 934, `http://www.esi.ac.at` (2000).

[9] L. Borcea, J.G. Berryman and G. Papanicolaou, High-contrast impedance tomography, Inverse Problems 12(6) (1996) 835–858.

[10] C.M. Bowden, J.P. Dowling and H.O. Everitt, eds., Development and applications of materials exhibiting photonic band gaps, J. Optical Soc. Amer. B 10 (1993) 280–413.

[11] R. Carlson, Hill's equation for a homogeneous tree, Electronic J. Diff. Equations, No. 23 (1997) 1–30.

[12] R. Carlson, Adjoint and self-adjoint operators on graphs, Electronic J. Diff. Equations, No. 6 (1998) 1–10.

[13] R. Carlson, Inverse eigenvalue problems on directed graphs, Trans. Amer. Math. Soc. 351(10) (1999) 4069–4088.

[14] R. Carlson, Nonclassical Sturm–Liouville problems and Schrödinger operators on radial trees, Preprint (2000).
[15] J.M. Combes, Spectral problems in the theory of photonic crystals, in: *Mathematical Results in Quantum Mechanics (QMath7)*, Prague, 22–26 June 1998, eds. J. Dittrich et al., Operator Theory, Advances and Applications, Vol. 108 (Birkhäuser, Basel, 1999) pp. 33–46.
[16] S. Datta, *Electronic Transport in Mesoscopic Systems* (Cambridge Univ. Press, Cambridge, 1995).
[17] P.-G. de Gennes, Champ critique d'une boucle supraconductrice ramefiee, C. R. Acad. Sci. Paris B 292 (1981) 279–282.
[18] D.C. Dobson, An efficient method for band structure calculations in 2D photonic crystals, J. Comput. Phys. 149 (1999) 363–376.
[19] M.S.P. Eastham, *The Spectral Theory of Periodic Differential Equations* (Scottish Acad. Press, Edinburgh/London, 1973).
[20] W.D. Evans and D.J. Harris, Fractals, trees and the Neumann Laplacian, Math. Ann. 296 (1993) 493–527.
[21] W.D. Evans and Y. Saito, Neumann Laplacians on domains and operators on associated trees, to appear in Quart. J. Math. Oxford.
[22] P. Exner, Lattice Kronig–Penney models, Phys. Rev. Lett. 74 (1995) 3503–3506.
[23] P. Exner, Contact interactions on graph superlattices, J. Phys. A 29 (1996) 87–102.
[24] P. Exner and P. Seba, Electrons in semiconductor microstructures: a challenge to operator theorists, in: *Proceedings of the Workshop on Schrödinger Operators, Standard and Nonstandard*, Dubna, 1988 (World Scientific, Singapore, 1989) pp. 79–100.
[25] A. Figotin, High-contrast photonic crystals, in: *Diffuse Waves in Complex Media*, Les Houches, 1998, NATO Advanced Science Institutes Series C: Mathematical and Physical Sciences, Vol. 531 (Kluwer Academic, Dordrecht, 1999) pp. 109–136.
[26] A. Figotin and Y. Godin, The computation of spectra of some 2D photonic crystals, J. Comput. Phys. 136 (1997) 585–598.
[27] A. Figotin and P. Kuchment, Band-gap structure of the spectrum of periodic and acoustic media. I. Scalar model, SIAM J. Appl. Math. 56(1) (1996) 68–88.
[28] A. Figotin and P. Kuchment, Band-gap structure of the spectrum of periodic and acoustic media. II. 2D photonic crystals, SIAM J. Appl. Math. 56 (1996) 1561–1620.
[29] A. Figotin and P. Kuchment, 2D photonic crystals with cubic structure: Asymptotic analysis, in: *Wave Propagation in Complex Media*, ed. G. Papanicolaou, The IMA Volumes in Mathematics and its Applications, Vol. 96 (1997) pp. 23–30.
[30] A. Figotin and P. Kuchment, Spectral properties of classical waves in high contrast periodic media, SIAM J. Appl. Math. 58(2) (1998) 683–702.
[31] A. Figotin and P. Kuchment, Asymptotic models of high contrast periodic photonic and acoustic media (tentative title), parts I and II, in preparation.
[32] M. Freidlin, *Markov Processes and Differential Equations: Asymptotic Problems*, Lectures in Mathematics, ETH Zürich (Birkhäuser, Basel, 1996).
[33] M. Freidlin and A. Wentzell, Diffusion processes on graphs and the averaging principle, Ann. Probab. 21(4) (1993) 2215–2245.
[34] N. Gerasimenko and B. Pavlov, Scattering problems on non-compact graphs, Theoret. Math. Phys. 75 (1988) 230–240.
[35] C. Giovannella and C.J. Lambert, eds., *Lectures on Superconductivity in Networks and Mesoscopic Systems*, AIP Conference Proceedings, Vol. 427, Pontignano, Italy, September 1997 (Amer. Inst. of Physics, 1998).
[36] J.S. Griffith, A free-electron theory of conjugated molecules. I. Polycyclic hydrocarbons, Trans. Faraday Soc. 49 (1953) 345–351.
[37] J.S. Griffith, A free-electron theory of conjugated molecules. II. A derived algebraic scheme, Proc. Cambridge Philos. Soc. 49 (1953) 650–658.

[38] P. Grisvard, *Elliptic Problems in Nonsmooth Domains*, Monographs and Studies in Mathematics, Vol. 24 (Advanced Publishing Program) (Pitman, Boston, MA, 1985).

[39] P.M. Hui and N.F. Johnson, Photonic band-gap materials, in: *Solid State Physics*, Vol. 49, eds. H. Ehrenreich and F. Spaepen (Academic Press, New York, 1995) pp. 151–203.

[40] Y. Imry, *Introduction to Mesoscopic Physics (Mesoscopic Physics and Nanotechnology)* (Oxford Univ. Press, Oxford, 1997).

[41] K. Inoue, M. Sasada, J. Kuwamata, K. Sakoda and J.W. Haus, A two-dimensional photonic crystal laser, Japan J. Appl. Phys.

[42] J.D. Jackson, *Classical Electrodynamics* (Wiley, New York, 1962).

[43] C. Joachim and S. Roth, eds., *Atomic and Molecular Wires*, NATO Advanced Science Institutes Series E: Applied Sciences, Vol. 341 (Kluwer, Dordrecht, 1997).

[44] J.D. Joannopoulos, R.D. Meade and J.N. Winn, *Photonic Crystals, Molding the Flow of Light* (Princeton Univ. Press, Princeton, NJ, 1995).

[45] S. John, Strong localization of photons in certain disordered dielectric superlattices, Phys. Rev. Lett. 58 (1987) 2486.

[46] V.A. Kondrat'ev and O.A. Oleinik, Boundary value problems for partial differential equations in nonsmooth domains (in Russian), Uspekhi Mat. Nauk 382(230) (1983) 3–76.

[47] V. Kostrykin and R. Schrader, Kirchhoff's rule for quantum wires, J. Phys. A 32(1999) 595–630.

[48] V. Kostrykin and R. Schrader, Kirchhoff's rule for quantum wires. II: The inverse problem with possible applications to quantum computers, Preprint (2000).

[49] P. Kuchment, *Floquet Theory for Partial Differential Equations* (Birkhäuser, Basel, 1993).

[50] P. Kuchment, The mathematics of photonics crystals, in: *Mathematical Modeling in Optical Science*, chapter 7, eds. G. Bao, L. Cowsar and W. Masters, Frontiers in Applied Mathematics, Vol. 22 (SIAM, Philadelphia, PA, 2001).

[51] P. Kuchment and L. Kunyansky, Spectral properties of high contrast band-gap materials and operators on graphs, Experiment. Math. 8(1) (1999) 1–28.

[52] P. Kuchment and H. Zeng, Convergence of spectra of mesoscopic systems collapsing onto a graph, J. Math. Anal. Appl. 258 (2001) 671–700.

[53] G. Kurizki and J. W. Haus, eds., *Photonic Band Structures,* J. Modern Optics 41(2) (1994), a special issue.

[54] S. Novikov, Schrödinger operators on graphs and topology, Russian Math. Surveys 52(6) (1997) 177–178.

[55] S. Novikov, Discrete Schrödinger operators and topology, Asian Math. J. 2(4) (1999) 841–853.

[56] S. Novikov, Schrödinger operators on graphs and symplectic geometry, in: *The Arnoldfest*, Toronto, ON, 1997, Fields Institute Communications 24 (Amer. Math. Soc., Providence, RI, 1999) pp. 397–413.

[57] Photonic & Acoustic Band-Gap Bibliography, `http://www.ee.ucla.edu/labs/photon/biblio.html`.

[58] J. Rarity and C. Weisbuch, eds., *Microcavities and Photonic Bandgaps: Physics and Applications, Proceedings of the NATO Advanced Study Institute: Quantum Optics in Wavelength-Scale Structures*, Cargese, Corsica, 26 August–2 September 1995, NATO Advanced Science Institutes Series (Kluwer Academic, Dordrecht, 1996).

[59] M. Reed and B. Simon, *Methods of Modern Mathematical Physics*, Vol. IV: *Analysis of Operators*, (Academic Press, New York, 1978).

[60] J. Rubinstein and M. Schatzman, Spectral and variational problems on multiconnected strips, C. R. Acad. Sci. Paris Ser. I Math. 325(4) (1997) 377–382.

[61] J. Rubinstein and M. Schatzman, Asymptotics for thin superconducting rings, J. Math. Pures Appl. (9) 77(8) (1998) 801–820.

[62] J. Rubinstein and M. Schatzman, On multiply connected mesoscopic superconducting structures, Sémin. Théor. Spectr. Géom., No. 15, Université Grenoble I, Saint-Martin-d'Hères (1998) 207–220.

[63] J. Rubinstein and M. Schatzman, Variational problems on multiply connected thin strips I: Basic estimates and convergence of the Laplacian spectrum, Preprint (1999).
[64] K. Ruedenberg and C.W. Scherr, Free-electron network model for conjugated systems. I. Theory, J. Chem. Phys. 21(9) (1953) 1565–1581.
[65] Y. Saito, The limiting equation of the Neumann Laplacians on shrinking domains, Preprint (1999).
[66] M. Schatzman, On the eigenvalues of the Laplace operator on a thin set with Neumann boundary conditions, Appl. Anal. 61 (1996) 293–306.
[67] M. Scheffler and R. Zimmermann, eds., *The Physics of Semiconductors, Proceedings of 23rd Internat. Conf.*, Vol. 2, Berlin, 21–26 July 1996 (World Scientific, Singapore, 1996).
[68] P.A. Serena and N. Garcia, eds., *Nanowires*, NATO Advanced Science Institutes Series E: Applied Sciences, Vol. 340 (Kluwer, Dordrecht, 1997).
[69] C.M. Soukoulis, ed., *Photonic Band Gap Materials, Proceedings of the NATO Advanced Science Institutes on Photonic Band Gap Materials*, Elounda, Crete, Greece, 18–30 June 1995, NATO Advanced Science Institutes Series (Kluwer Academic, Dordrecht, 1996).
[70] P.R. Villaneuve and M. Piché, Photonic band gaps in periodic dielectric structures, Progress Quant. Electr. 18 (1994) 153–200.
[71] E. Yablonovitch, Inhibited spontaneous emission in solid-state physics and electronics, Phys. Rev. Lett. 58 (1987) 2059 .